This is the author's version of an article that has been published in this journal. Changes were made to this version by the publisher prior to publication.
The final version of record is available at http://dx.doi.org/10.1109/TASC.2017.2658951

Design of 4 Tm Forward Dipoles for the FCC-hh Detector Magnet System

M. Mentink, H. Da Silva, A. Dudarev, G. Rolando, B. Cure, A. Gaddi, V. Klyukhin, H. Gerwig, U. Wagner, and H. ten Kate

***Abstract*—The 4 T, 10 m free bore Twin Solenoid with 4 Tm forward dipoles is discussed with an emphasis on the forward dipoles. This assembly, a possible detector magnet layout for the Future Circular Collider for hadron-hadron physics, combines a 4 T axial magnetic field at the interaction point in the center of the Twin Solenoid with off-axis magnetic fields generated by the two forward dipoles for the purpose of providing bending power to all particles emanating from the interaction point.**

The Twin Solenoid provides 4 T over a free bore diameter of 10 m, resulting in a stored energy of 15.4 GJ, a cold mass of 1.25 kt, and a vacuum vessel mass of 1.4 kt. This configuration leads to acceptable quench protection and mechanical properties.

The forward dipoles are located in the stray field of the Twin Solenoid, resulting in large forces and torques on the coils. Two forward dipole options are presented. In the first option, the main dipole coils are combined with lateral coils for the purpose of bringing the net force and torque on the cold mass to zero. In the second option, the lateral coils are omitted and the net force and torque is handled through the vacuum vessel. The first option results in a stored energy of 240 MJ, a cold mass of 250 tons, and a vacuum vessel of 150 tons, whereas the second options gives 130 MJ, 100 tons, and 180 tons, respectively.

The forward dipole conductor comprises copper and NbTi and is force-flow cooled with helium. The superconducting coils are placed in a stainless steel coil casing and pre-compressed. The coil casings are then fixed to the main body support structure, thus allowing transfer of forces and torques between the coils. The analyses indicate that this leads to good quench protection and mechanical behavior.

***Index Terms*—Superconducting magnet, detector, FCC-hh**

I. Introduction

AS part of the Future Circular Collider for hadron-hadron collisions (FCC-hh) study, CERN is developing new concepts for detectors featuring accurate characterization of particle products over a wide pseudorapidity range. Here the conceptual design of a 4 Tm forward dipole is discussed, to be used in combination with the "Twin Solenoid" design [1].

The combination of a solenoid-based main detector magnet with forward dipoles gives full pseudorapidity coverage. The solenoidal magnet provides efficient bending power for particles with trajectories travelling perpendicular to the beam, whereas the forward dipole provides bending power for particles travelling nearly parallel to the beam. However, the placement of forward dipoles in close proximity to the Twin Solenoid is challenging because the magnetic coupling between the magnets leads to large forces and torques on each of the coils.

All authors are affiliated with the FCC Detector Magnet Group at CERN. The primary author (email: mmentink@cern.ch) is with the ATLAS magnet group, Physics Department, CERN, 1217 Meyrin, Switzerland.

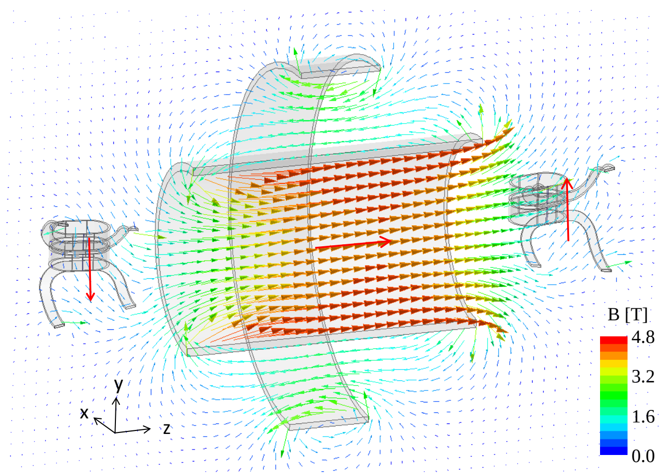

Fig. 1. Field map of the Twin Solenoid in combination with two Forward Dipoles. The solenoidal field generated by the Twin Solenoid is favorable for bending low-pseudorapidity particles, while the dipole field generated by the Forward Dipoles is favorable for high-pseudorapidity particles.

The forces and torques may be handled in two different ways. Firstly, one may accept the forces and torques on the cold mass, and seek to mitigate them through the support structure. Secondly, one may utilize a novel coil configuration to reduce the net force and torque to zero as previously suggested [1]. In this paper, both options are considered, with emphasis on the latter.

The Twin Solenoid is discussed in section II. The difference with the previous version [1] is that the magnetic field over the bore is reduced to 4 T and the free bore diameter is reduced to 10 m, rather than the 6 T/12 m system studied before. The concept of the Force-and-Torque-Neutral Forward Dipole is discussed in section III. The material choices and conductor geometry for the forward dipole are discussed in section IV. The procedures for manufacturing the coils and integrating them with the support structure are outlined in section V. Magnetic and mechanical simulations are performed to determine resulting stresses and results are shown in section VI. A conceptual design of the vacuum vessel is presented in section VII. The quench behavior is discussed in section VIII. The implications of omitting the lateral coils entirely are discussed in section IX. Finally, this is followed by a discussion in section X and conclusion in section XI.

II. 4 T/10 m Twin Solenoid Detector Magnet

Fig. 1 shows the magnetic field generated by the Twin Solenoid and the Force-and-Torque-Neutral Forward Dipoles.

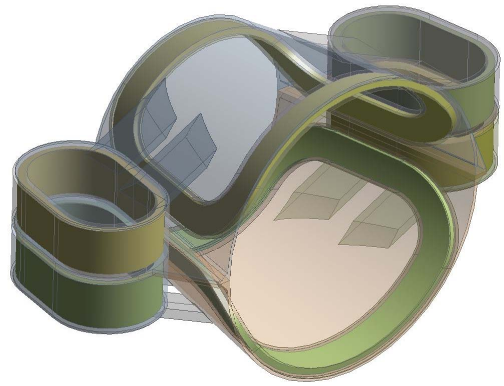

Fig. 2. Schematic representation of the cold mass of the Force-and-Torque-Neutral dipole. Here the coils are indicated in green and the support structure is transparent.

TABLE I
4 T/10 M TWIN SOLENOID AND 4 TM FORWARD DIPOLE GENERAL PROPERTIES

	Twin Solenoid	Force and Torque Neutral Dipole	Unbalanced Dipole
Stored energy [GJ]	15.4	0.24	0.13
Operating current [kA]	47	16.6	16.6
Self-Inductance [H]	14	1.7	1.0
Current density [A/mm^2]	9.9	30.6	30.6
Conductor length [km]	85	15	8
Conductor mass [t]	1080	65	34
Support structure mass [t]	180	187	68
Total cold mass [t]	1250	250	102
Vacuum vessel mass [t]	1400	150	180

Here, the inner coil of the Twin Solenoid generates a magnetic field over the free bore and the outer coil returns the magnetic flux generated by the inner coil, thus reducing the stray field and facilitating muon tagging. For the purpose of reducing the overall cost of the system, the Twin Solenoid is reduced in size and magnetic field strength in comparison to previous versions, now generating a magnetic field of 4 T over a free bore of 10 m. A minimum shaft diameter of 23.5 m is needed to lower the Twin Solenoid down to the detector cavern. The 5 mT boundary, indicative of the overall stray field of the Twin Solenoid, is located 24 meters away from the interaction point in the radial direction and 47 meters in the axial direction.

The conductor used for the Twin Solenoid is an aluminum-stabilized Rutherford cable, operating at 47 kA, with dimensions of 80 and 59 mm in the axial and radial directions, respectively, which includes 1 mm fiberglass insulation between conductors and 2 mm insulation to ground. The residual resistivity ratio is assumed equal to 400. The inner solenoid then comprises 220×8 turns in addition to a 50 mm thick support cylinder and the outer solenoid comprises 60×6 turns and a 100 mm thick support cylinder. The superconducting Rutherford cable in the center of this conductor is fabricated from 64×1.5 mm diameter NbTi/Cu strands. The peak field on the conductor is 4.7 T (a homogeneous current distribution in the winding gives 4.2 T). The resulting current sharing temperature is 6.4 K, i.e. 1.9 K above the expected operating temperature of 4.5 K. For comparison, the Compact Muon Solenoid and the ATLAS barrel toroid conductors were designed with current sharing temperatures of 6.5 K and 6.4 K, respectively [6], [7].

Quench simulations are performed with Quench 2.7 [2] to evaluate the expected quench behavior under normal and fault conditions and these simulations indicate that this magnet has acceptable quench behavior. Under normal conditions where a quench is detected within seconds, normal zones are induced with quench heaters, and the magnet is discharged over a 21 mΩ dump resistor (resulting in a peak discharge voltage of 1000 V), 70% of the stored magnetic energy is dissipated over the dump resistor and the expected peak hot spot temperature in the cold mass is 64 K. In this case it takes about 15 minutes for the current to drop by a factor 10. Here, the combination of both quench heaters and energy extraction provides fault tolerance. Malfunctioning of either the quench heaters or energy extraction results in hot spot temperatures of 65 K and 96 K, respectively. In the worst-case fault scenario where neither quench heating nor energy extraction is applied, the hot spot temperature reaches 183 K. In all cases the worst-case layer-to-layer voltage is 270 V, and the worst-case coil-to-ground voltage is 1000 V.

The mechanical stress in the conductor is a function of the elastic behavior of the conductor. Assuming that the conductor comprises nickel-doped aluminum with a yield stress well above 100 MPa [3], and using COMSOL Multiphysics for mechanical calculations, a peak stress of 93 MPa was found in the windings of the Twin Solenoid. Nickel-doped aluminum was used in the ATLAS central solenoid, albeit in a conductor with much smaller dimensions [4], resulting in a conductor with a yield strength of 146 MPa. An alternative is the conductor technology used for the Compact Muon Solenoid [5], combining pure aluminum for good electrical and thermal properties and aluminum alloy for good mechanical properties. Either of these concepts seems feasible, although the implications of applying either technology to a conductor with the appropriate dimensions are presently not fully understood.

The vacuum vessel of the Twin Solenoid weighs 1.4 kt. The same (rather conservative) radiation heat load assumptions are taken as for the Technical Design Report of the Compact Muon Solenoid [6], given a total radiation heat load of 7100 W onto the 50 K thermal shield and 476 W onto the cold mass. In addition, 760 W is needed to keep the thermalization points of the tie rods at 50 K, and 5.8 W of heat goes towards the cold mass.

III. 4 TM FORCE-AND-TORQUE-NEUTRAL FORWARD DIPOLE

The Force-and-Torque-Neutral dipole (Fig. 2) combines main dipole coils and lateral dipole coils. The main dipole coils surround the free bore, which is sufficiently large for particles with pseudorapidity η equal or larger than 2.5 to pass through. The lateral coils return the magnetic flux generated by the main dipole coils and bring the net force and torque on the cold mass to zero. In addition, the lateral coils contribute about 25% of the field integral inside the free bore of the forward dipole.

Similarly to the Twin Solenoid, the Force-and-Torque-Neutral dipole is scaled down in terms of magnetic field strength. It now produces a field integral of 4 Tm for particles at pseudorapidities equal to or exceeding 2.5. The field in the center is about 0.9 T.

IV. Dipole Material Choices and Conductor Geometry

The conductor of the Forward Dipole comprises copper stabilizer in addition to Cu/NbTi wires and the support structure is made out of stainless steel. There are a number of motivations for these choices. Firstly, the Forward Dipole comprises a number of complex shapes, and using stainless steel allows for more flexibility with regards to welding. The thermal contraction of the stainless steel is very similar to that of copper, so thermal stress may be avoided with this material combination. Secondly, various concepts utilized for this design are loosely based on the Morpurgo superconducting dipole, one of the largest superconducting dipoles ever built [8], for which also this combination of materials was used.

Given the poor thermal conductivity of stainless steel, internal cooling is used to maintain the operating temperature. Fig. 3 shows the superconducting conductor, which is based on the conductor used for the Morpurgo superconducting dipole. Here, 32 1.25 mm diameter NbTi/Cu strands are wound onto a copper tube. Subsequently, two copper U-profiles encapsulate the copper tube and the strands. This assembly is then soldered together using a low-temperature solder. The outer dimensions are 24 and 23 mm for the main dipole coils, and 25 and 22 mm for the lateral coils, where 1 mm fiberglass insulation between neighboring conductors is included in these numbers.

When energized, the peak field on the conductor is 5.1 T, i.e. 0.25 T of which is due to the concentrated distribution of current inside the conductor (Fig. 3). Assuming an equal amount of copper and NbTi in the strands, the current sharing temperature of the conductor is 6.2 K, i.e. 1.7 K above the operating temperature of 4.5 K. Given the excellent thermal contact between strands and coolant, this temperature margin is considered sufficient.

V. Coil Manufacture and Integration with Support Structure

Due to the relatively low stored energy in comparison to the Twin Solenoid, the current density in the dipole conductor is over three times higher than in the Twin Solenoid (Table I). This means that for the purpose of quench protection the Twin Solenoid and Forward Dipoles are necessarily in a different electrical circuit, where any combination of current in the Twin Solenoid and Forward Dipole should be considered for the purpose of Lorentz forces on the dipole conductor. The field orientation on the coils of the Forward Dipole is then given by any possible combination of current in the Twin Solenoid and the Forward Dipole itself, meaning that the Lorentz force cannot just vary significantly in magnitude, but also in direction.

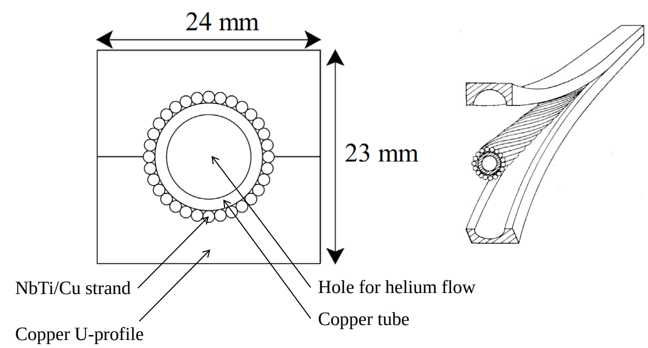

Fig. 3. Left: Schematic representation of the conductor used for the Forward Dipole. Right: Schematic representation of the conductor used for the Morpurgo superconducting dipole, also showing the copper tube, the winded NbTi/Cu strands, and the two copper U-profiles.

To avoid sudden movement of the conductor resulting in a quench, it is important that the coils are pre-compressed. The assembly procedure is based on the process used for the Wendelstein 7-X Stellerator [9] and is as follows:

Firstly, the conductor is wound on a winding fixture and the coil pack is epoxy-impregnated. Secondly, a stainless steel coil casing is placed over the coil pack and welded shut. Thirdly, the stainless steel casing is heated and the space in between the coil and casing is filled with a mixture of quartz sand and resin. Finally, the casing is closed and allowed to cool down, so that thermal shrinkage of the coil casing results in pre-compression of the coil windings.

The main support frame comprises a half shell welded to side plates for the lateral dipole coils. Firstly, the main dipole coils and surrounding coil casings are placed inside the half shell, bolted to the support frame, and subsequently welded. Subsequently, the two half shells are bolted and welded together. The lateral coils are then placed on the side plates, and the top support frames are placed on top. After these are bolted together, a final welding stage ensures proper mechanical support between all elements. The various elements and the completed assembly are shown in Figs. 4 and 2, respectively.

VI. Resulting Stresses

Two different types of simulations are performed to determine the resulting stresses for the given geometry. In both simulations ANSYS static structural analysis was used.

Both the Forward Dipoles and the Twin Solenoid are assumed to be fully energized. Note that this is the worst case scenario. For instance, the interaction of the conductor in the main dipole coils with the stray field of the Twin Solenoid results in a force away from the conical support structure in one of the main dipole coils and towards the conical support structure in the other, so that the total peak stress in indicative of the worst case scenario.

The coils are assumed to be mechanically homogeneous, i.e. no cutouts were made for the hollow tube in the center of the conductor (Fig. 3), but the elastic modulus of the copper,

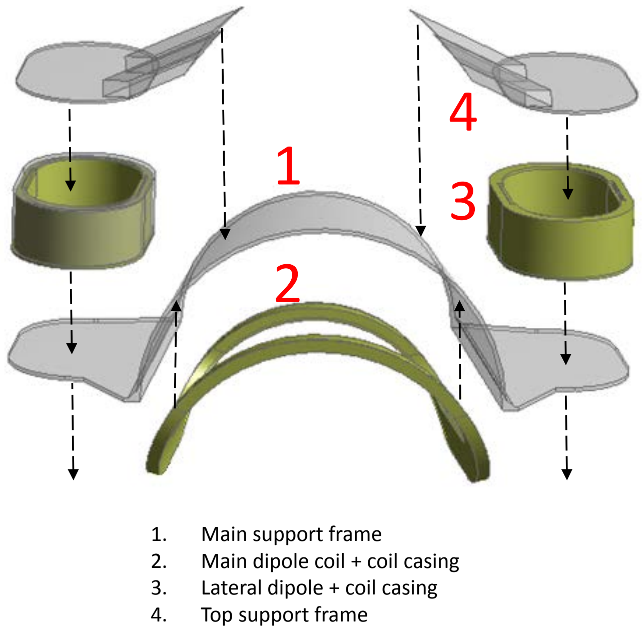

Fig. 4. Components of the Force-and-torque-neutral Dipole. Here, the superconducting coils and coil casings are indicated in green and the support structure is indicated in grey. The complete cold mass comprises two assembled elements as shown here.

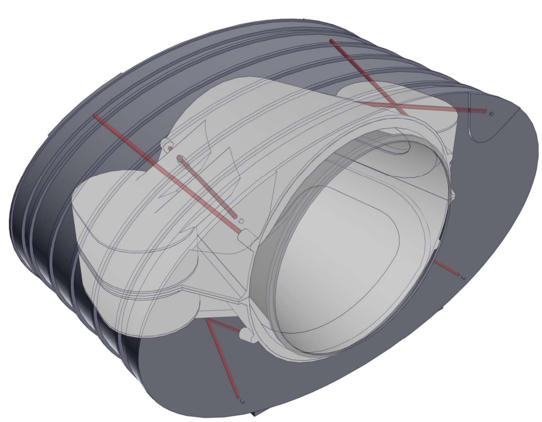

Fig. 5. Schematic representation of the vacuum vessel of the Force-and-Torque-Neutral dipole. The tie rods between the cold mass and the vacuum vessel are indicated in red.

normally about 140 MPa at cryogenic temperature [10], was reduced by 12% to account for the hollow center. The elastic modulus of the 304 stainless steel is 180 MPa [11].

In the first simulation, all coils are fully bonded to the surrounding support structure, leading to a peak Von Mises stress of 65 MPa in the coils themselves, 120 MPa in the surrounding coil casings, and 110 MPa in the main support structure.

A potential problem with assuming full bonding is that the local stress on the interface between the coil and support structure may exceed the maximum allowed stress on the epoxy. Therefore, in the second simulation, the coils are not bonded to the coil casings, but are free to move. In addition, the coils are chamfered to avoid local stress concentrations. The peak stress is then no longer a function of the overall support structure, but primarily of the support structure located in the direction that the coils expand towards. For instance, in the case of the lateral racetrack coils this signifies the support structure on the outside of the coil. With a support structure thickness of 100 mm, the peak stress on the coil itself is 120 MPa and the peak stress on the coil casing is 165 MPa, i.e. higher than in the fully bonded case.

These levels of stresses are acceptable. Using 80 K as a reference (to allow for local temperature increases resulting from a quench), the yield strength and ultimate tensile strength of half-hard copper are 400 and 500 MPa, respectively, which implies a maximum allowed stress of about 170 MPa, i.e. one-third of the ultimate tensile strength. For annealed stainless steel 304, the yield strength and ultimate tensile strength are 400 and 1600 MPa, thus implying a maximum allowed stress of 270 MPa, i.e. two-third of the yield strength.

The peak stress on the stainless steel is well below the maximum allowed stress, thus implying that the weight of the support structure may yet be made somewhat lighter. For the copper conductor, the stress is about appropriate when considering that the hollow tubes in the centers of the conductors are not incorporated in the simulation, thus implying an increase in local stress. It is possible that incorporating the hollow cores may result in stress exceeding the indicated limits, but some plasticity seems acceptable given that the stainless steel casings will guarantee the overall structural integrity of the coil.

A more critical issue is the local stress on the epoxy. When the coil is glued into the coil casing, energizing the magnet may lead to substantial shear stress on the glued interfaces. Thus, it is preferable to only allow gluing of the interfaces that are compressed when the magnet is energized (for instances, the outside surfaces of the lateral coils). The resulting stresses then correspond to the simulation in which the coil is free to move. This approach, combined with pre-compression to close any gaps present after fabrication should be sufficient to achieve the desired transfer of forces between coils without the risk of sudden coil movement and epoxy cracking. An alternative approach is to glue all interfaces between coil and coil casing, but in this case it is critical that the level of pre-compression is sufficient to prevent the coil from shearing off the coil casing when the magnet is energized.

VII. Vacuum Vessel

Fig. 5 shows a schematic representation of the vacuum vessel. The vacuum vessel is oval-shaped to accommodate the unusual shape of the cold mass. The outer shell is made of stainless steel 304L (chosen for improved weldability) and the overall weight is 150 tons. The radiation heat loads on the thermal shield and cold mass are 1100 W and 74 W, respectively.

Assuming a maximum allowed tensile stress of 600 MPa on the titanium tie-rods, the top tie rods have a diameter of 100 mm and the bottom ones 70 mm. The length of the tie rods is 5 m. Assuming thermalization at 50 K, the total heat load on the cold mass is 0.86 W and the total heat load to 50 K is 170 W. The vacuum vessel and tie rods are sufficiently strong to handle a seismic event of 0.15 times gravity and a cold mass misplacement of 10 mm in any direction.

VIII. Quench protection of the forward dipole

The amount of coil mass is chosen to achieve reasonable hot spot temperatures even under adverse conditions. The volume of the coils is 8.2 m^3, which corresponds to a mass of 65 tons. Given the poor thermal conductivity of stainless steel, the thermal behavior of the surrounding stainless steel support structure is not considered here.

In the best case scenario the dipole is discharged over a 30 mΩ resistor (leading to an initial discharge voltage of 500 V per dipole) while simultaneously experiencing a homogeneous quench. This homogeneous quench may for instance be achieved by heating up the coolant near the inlet of the coils. Assuming a RRR of 80, this leads to a hot spot temperature of 53 K. In the case where energy extraction does not work, this number increases to 68 K. One may also consider a fault scenario where quench heating is not applied and the normal zone propagates through the coil very slowly. Such an event may occur when the normal zone is propagating against the flow of the coolant, for instance originating from a bus bar near the helium exhaust. In this case, one may assume that the conductor is adiabatically heated while the dipole is discharging over the dump resistor, leading to a hot spot temperature of 79 K.

IX. Forward dipole without lateral coils

To evaluate the cost of force and torque neutrality, an evaluation is done of a 4 Tm dipole without the lateral coils. Omitting these coils leads to a reduction in stored energy to 130 MJ, but also a net torque over the x-axis of 63 MNm and an upward force of 9.7 MN. The overall coil volume is then reduced to 4.2 m^3 for a total weight of 34 tons and the support structure weight is reduced to 68 tons.

Even though the volume of the cold mass decreases, the mass of the vacuum mass increases to 180 tons due to the reinforcement needed to handle the forces and torques. The radiation heat loads to the thermal shield and cold mass drop to 850 and 57 W, respectively. The conduction heat loads through the rods are now 200 and 2.3 W for the heat shield and cold mass respectively. Even though the heat load through the tie-rods is higher compared to the Force-and-Torque-Neutral dipole, the total heat load is dominated by radiation load. The total heat load of 59 W is about 20% lower in comparison to the Force-and-Torque-Neutral dipole.

X. Discussion

In the original Wendelstein 7-X mounting procedure, the stainless steel casing was heated up to 120 degrees centigrade to overcome the difference in thermal contraction between the stainless steel casing and the aluminum conductor. Given the thermal match between stainless steel and copper used for the Forward Dipole, such a high temperature might not be required, but further study is needed to find the appropriate procedure.

Given that the Wendelstein superconducting coils combined aluminum with stainless steel support structure, one may argue that the same material combination may be used here. Indeed, either option is likely to work. The options for copper does seem attractive because it is believed to be easier to use with regards to fabrication of gas-tight joints.

With regards to the choice between a compensated and uncompensated coil, different arguments may be given for either option. Clearly it is attractive to reduce the net force and torque on the cold mass to zero, as it implies minimal additional constraints on the detector cavern infrastructure. At the same time, this option is more costly in terms of construction and, perhaps counter-intuitively, in terms of the required cooling power. Making a choice between these two options is beyond the scope of this paper, which is why both options are presented here.

XI. Conclusion

A revised version of the Twin Solenoid and Forward Dipole design, part of a design study for a detector intended for FCC-hh, is presented here. The magnets are scaled down in magnetic field and size, so that the Twin Solenoid provides 4 T over a 10 m free bore and the Forward Dipole provides 4 Tm of bending power for particles at pseudorapidities equal to or exceeding 2.5.

The proximity of the Forward Dipole to the Twin Solenoid results in very large net forces and torques in the individual coils. This issue may be resolved in two different ways. Firstly, one may accept a non-zero net force and torque on the cold mass and adjust the support structure accordingly, or one may use a special geometry comprising main and lateral dipole coils, where the net force and torque on the cold mass is equal to zero. The latter options results in a stored energy of 240 MJ, a cold mass of 250 tons, and a vacuum vessel mass of 150 tons, whereas the former options results in about half the stored energy and cold mass, and a comparable vacuum vessel weight. Despite the very high net force and torque in case of the uncompensated Forward Dipole of 65 MNm and 9.7 MN respectively, this option is more efficient from a cooling perspective. This somewhat surprising result is due to a smaller vacuum vessel size in the case of the uncompensated Forward Dipole, thus reducing the radiation heat load, in combination with thermally efficient titanium tie rods.

A copper-stabilizer-based force-flow-cooled conductor is used in combination with a stainless steel support structure. A pre-compression technique is used to allow for the transferal of large forces and torques between the coils and the support structure. The mechanical properties and quench behavior of both the Twin Solenoid and the Forward Dipole are investigated and the results indicate acceptable values.

References

[1] M. Mentink, A. Dudarev, H. Da Silva, C. Berriaud, G. Rolando, R. Pots, B. Cure, A. Gaddi, V. Klyukhin, H. Gerwig, U. Wagner, and H. ten Kate, "Design of a 56-GJ Twin Solenoid and Dipoles Detector Magnet System for the Future Circular Collider", *IEEE Trans. on Appl. Supercond.* 26, 4003506 (2016).

[2] J. van Nugteren, A. Dudarev, M. Dhalle, and H. ten Kate, "Software development for the science and design behind superconducting magnet systems", Internship report, CERN (2011)

[3] K. Wada, S. Meguro, H. Sakamoto, A. Yamamoto, and Y. Makida, "High-strength and High-RRR Al-Ni Alloy for Aluminum-Stabilized Superconductor", *IEEE Trans. on Appl. Supercond.* 10, p. 1012 (2000).

[4] A. Yamamoto, T. Kondo, Y. Doi, Y. Maki, T. Tanaka, T. Haruyama, H. Yamaoka, H. H. J. ten Kate, L. Bjorset, K. Wada, S. Meguro, J. S. H. Ross, and K. D. Smith, "Design and Development of the ATLAS Central Solenoid Magnet", *IEEE Trans. on Appl. Supercond.* 9, pp. 852-855 (1999).

[5] B. Cure, B. Blau, A. Herve, P. Riboni, S. Tavares and S. Sgobba, "Mechanical Properties of the CMS Conductor", *IEEE Trans. on Appl. Supercond.* 14, p. 530 (2004)

[6] CMS Collaboration, "CMS, the Magnet Project", Technical Design Report (1997).

[7] ATLAS Magnet Project Collaboration, "Barrel Toroid, Magnet Project TDR Volume 2", Technical Design Report (1997).

[8] M. Morpurgo, "A large superconducting dipole cooled by forced circulation of two phase helium", *Cryogenics*, 411 (1979).

[9] M. Endler, T. Bräuer, T. Kluck, J. Müller, and L. Wegener, "Measurements investigating the embedding procedure of the Wendelstein 7-X non-planar coils", *Fusion Eng. and Design* 84, 743-746 (2009).

[10] Copper Development Association Inc., "Cryogenic properties of copper", *https://www.copper.org/resources/properties/cryogenic/*.

[11] Nickel Development Institute, "Materials for cryogenic service, engineering properties of austenitic stainless steel", Pub. 4368 (1974).